

Temperature dependence of the sublattice spontaneous magnetization of $\text{YBa}_2\text{Cu}_3\text{O}_6$

Cesare Bucci, Pietro Carretta, Roberto De Renzi, Germano Guidi, SeungGyo Jang, Enrico Rastelli, Armando Tassi, and Marco Varotto

Dipartimento di Fisica, Università di Parma, I 43100 Parma, Italy

(Received 8 March 1993)

Zero-field copper NMR measurements on $\text{YBa}_2\text{Cu}_3\text{O}_6$ up to 380 K are reported. The temperature dependence of the local magnetic moment at the Cu(2) plane site is compared with the predictions of spin-wave theory, based on the exchange coupling constants obtained from inelastic neutron scattering. The agreement is satisfactory, within the limits of the theoretical approximations, but discrepancies with elastic neutron-scattering results are pointed out and justified in terms of three-dimensional stacking defects.

I. INTRODUCTION

It is well known that $\text{YBa}_2\text{Cu}_3\text{O}_{6+x}$ exhibits magnetic ordering when the oxygen content is kept in the range $0 < x < 0.4$; on the experimental side, static and dynamic magnetic properties are widely investigated by means of classical macroscopic methods as well as by a variety of microscopic probes, the main goal being the understanding of the mechanisms by which the addition of oxygen disrupts the magnetic order and correlations; on the theoretical side, models are studied to provide a quantum and statistical frame to the above-mentioned phenomenology.

At one end of the phase diagram the pure magnetic system ($\text{YBa}_2\text{Cu}_3\text{O}_6$), which is being perturbed by extra oxygen, is assumed to be a two-dimensional antiferromagnet with weak planar anisotropy and weak inter-plane interactions. Inelastic neutron scattering yielded conspicuous evidence in favor of this structure and indeed predictions for T_N based on this model, which use the measured values for the inter- and intra-plane exchange constants, agree with the observed Néel temperatures. On the other hand, another important feature of this magnetic system, the sublattice spontaneous magnetization $M(T)$, one of the most direct parameters that reflects the nature of the spin interactions as well as of their excitations, still needs to be measured with sufficient accuracy in order to establish the pertinence of the assumed model to $\text{YBa}_2\text{Cu}_3\text{O}_6$.

The presently available data regarding $M(T)$ come from nonlocal probes as in neutron diffraction (Refs. 1 and 2), as well as from muon-spin resonance (μSR) (Refs. 3 and 4) and zero-field NMR (limited to low temperatures) (Refs. 5–7), which are local probes.

μSR experiments yield in principle the spontaneous magnetization in a straightforward way,³ but in all the cuprous perovskites in the magnetic phase one finds systematic anomalies at low temperatures that are still under investigation and appear to be associated to the high sensitivity of the muon localization in relation to defects.^{4,8}

Regarding zero-field NMR experiments for Cu nuclei in the bilayers, Cu(2), the present situation is more promising: The accurate determination of the hyperfine

parameters (electric-field gradients and magnetic hyperfine constants, both independent of temperature and oxygen content⁹) allows one to determine the on-site static average magnetic moment within a constant factor. The two magnetic sublattices are indistinguishable in zero external field measurements. In three-dimensional (3D) ordered systems the zero-field NMR measurement is expected to be strictly proportional to the macroscopic sublattice magnetization as determined by elastic neutron scattering (ENS) from the integrated intensity under a Bragg peak; in this frame of reference, the comparison between the present results and ENS data will reveal interesting differences.

The main motivation for the present zero-field NMR experiment stems from the fact previous experiments on nominally $\text{YBa}_2\text{Cu}_3\text{O}_6$ systems⁷ lost the NMR signal above temperatures as low as 77 K, which limited the discussion to that temperature range. Under the assumption that the loss of NMR signal could be ascribed to extremely short spin-lattice relaxation times and to electric-field-gradient inhomogeneity, we purposely prepared highly reduced samples for which the measured relaxation times were long enough to allow the detection of the NMR signal up to 380 K. Above this temperature the relaxation time of our spin-echo signal becomes too short as well and the signal is lost.

By means of the present experiments combined with the existing low-temperature data we aim to provide $M(T)$ data over a wide temperature range which does not include the phase transition at T_N but certainly represent a valid test for model calculations. As a first step, we will discuss in this paper the validity of the spin-wave approximation along similar lines to the analysis presented when the neutron-diffraction data appeared.¹⁰

Possible causes of the small but systematic discrepancies between NMR and ENS data will be discussed.

II. EXPERIMENTAL DETAILS

The sample used in this experiment was prepared by solid-state reaction; the final reduction to $\text{YBa}_2\text{Cu}_3\text{O}_6$ was obtained by annealing for a few days in vacuum at 650°C and its tetragonal structure was characterized by

x-ray diffraction. In the antiferromagnetically ordered state, the nuclear resonance of the two Cu families is very different.

Cu(1)—Since the chains do not present any static magnetic order, and the magnetic field generated by the neighboring ordered bilayers cancels out at the Cu(1) positions, their nuclei are observed in quadrupolar resonance (NQR) near 30 MHz as shown in Fig. 1. Narrow lines and a long spin-lattice relaxation time T_1 are indication of a good homogeneity of the samples. The study of T_1 for Cu(1) as a function of temperature for different compositions in the antiferromagnetic range is interesting in relation to the dynamics of neighboring magnetic bilayers and is under way.

Cu(2)—The copper nuclei in the magnetic bilayers experience both a quadrupolar coupling to the electric-field gradient as is the case for Cu(1) and a Zeeman interaction with the hyperfine field generated by the atomic magnetic moments. The magnitude of the two interactions is such that the observed resonance in zero external field corresponds to the predictions of the *high magnetic field* approximation: As for the Cu nuclear spin $I = \frac{3}{2}$, one observes three transitions with selection rules $\Delta m = \pm 1$ whose separation is related to the quadrupolar interaction. The actual value of the Larmor frequency ν_L in the presence of the hyperfine field generated by the spontaneous sublattice magnetization is readily obtained from the measured spectrum (we include the third-order corrections as a standard procedure¹¹), as the relative orientation of the hyperfine field and the electric-field-gradient tensor can be determined from the site symmetry, in agreement with previous work.⁷

The resonance frequency ν_m due to the transitions ($m \leftrightarrow m-1$) are thus given by

$$\begin{aligned}\nu_{1/2} &= \nu_L [1 + (3/16)(\nu_Q/\nu_L)^2], \\ \nu_{-1/2} &= \nu_L [1 - (1/2)(\nu_Q/\nu_L) + (3/64)(\nu_Q/\nu_L)^3], \\ \nu_{3/2} &= \nu_L [1 + (1/2)(\nu_Q/\nu_L) - (3/64)(\nu_Q/\nu_L)^3].\end{aligned}\quad (1)$$

Zero-field NMR experiments were performed on a Bruker CXP 200-MHz spectrometer and on a custom

made solid-state apparatus. Partial inhomogeneous broadening recovery was obtained by the use of a $\pi/2$ - τ - π echo pulse sequence with a four-step cycling of the phases: $(xy+)(\bar{x}y-)(\bar{x}x+)(xx-)$, where x , $\bar{x} = -x$, and y refer to the transmission phases and the following sign to the acquisition phase.

This sequence produces an effective suppression of the magnetoacoustic *ringing*, which in turns allows the echo waiting time τ to be made as small as 11 μ sec. Such a short τ enables us to obtain satisfactory signal-to-noise ratio even when the transverse relaxation rate $1/T_2$ is very fast.

The temperature was stabilized and measured with a precision of ± 0.5 K. The frequency spectrum was measured at each temperature in order to detect the three main transitions for each Cu(2) isotope, as shown in Fig. 2. The relaxation times T_1 and T_2 were found depend weakly on temperature in the temperature range between 77 and 380 K: $T_2 = 8 \sim 30$ μ sec and $T_1 = 100 \sim 300$ μ sec. The present experiment was limited to liquid-nitrogen temperatures, but it overlaps with the data by Iwamoto *et al.*,⁷ which cover the lower temperatures.

III. RESULTS

The position of each peak in the experimental spectra is determined with an accuracy of about ± 200 KHz by fit with a Gaussian line shape. Equation (1) is then inverted to yield the values of ν_L and ν_Q from the frequency of the peaks. Within the uncertainty of each measurement, we find a nearly constant value for $\nu_Q = 23.5 \pm 0.4$ MHz, which agrees with the similar findings⁷ in the lower-temperature interval (1.5–77 K). Therefore the final values of $\nu_L(T)$ are obtained by setting $\nu_Q = 23.5$ MHz constant in the explored temperature interval (77–380 K). This choice is quite acceptable, since precision measurements of ν_Q indicate a small increase from 23.18 MHz (Ref. 6) at 4.2 K to 23.8 MHz at 505 K (Ref. 12), whose effect would be negligible in our analysis. Similar weak temperature dependences have been observed for the NQR frequency of Cu(1) (Fig. 1).

The temperature dependence of ν_L is shown in Fig. 3,

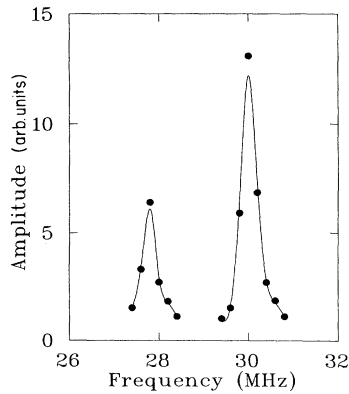


FIG. 1. Cu(1) NQR spectrum in $\text{YBa}_2\text{Cu}_3\text{O}_{6.05}$ at 150 K, obtained from the envelope of the echo amplitudes. The solid curve is a guide to the eye.

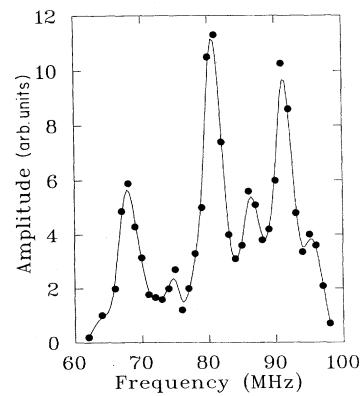


FIG. 2. Cu(2) antiferromagnetic nuclear resonance spectrum in $\text{YBa}_2\text{Cu}_3\text{O}_{6.05}$ at 200 K, obtained from the envelope of the echo amplitudes.

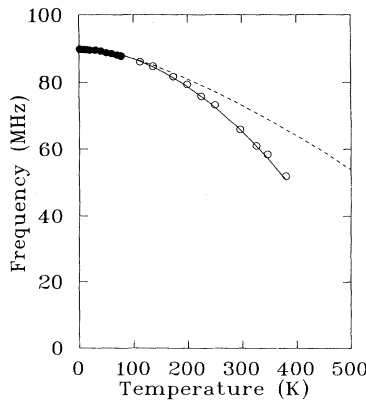


FIG. 3. Temperature dependence of the ^{63}Cu nuclear Zeeman frequencies ν_L . The solid line is the least-squares fitting derived from Eq. (2), with $\nu_L(0)=89.9$ MHz. The dashed line represents the comparison between NMR data and the predictions of Eq. (10).

together with the results reported in Ref. 7 for temperatures up to 77 K. It is remarkable that at 77 K the values provided by the two experiments coincide within the experimental errors of 0.4 MHz; this indicates that small differences in the oxygen content at these levels do not affect the value of the spontaneous magnetization. In view of the good matching of the two sets of data at 77 K we shall consider the range of temperatures between 1.5 and 380 K as a whole in the following part of the paper.

It is interesting to represent the same data on a log-log scale, plotting the reduction in $M(T)$, which is equal to $(\nu(0)-\nu(T))/\nu(0)$, as a function of T . To this purpose, the choice of $\nu(0)$ is important. Our extrapolation of the data for $T \rightarrow 0$ yields $\nu(0)=89.90$ MHz, consistent with the value of 89.8 ± 0.1 quoted by Ref. 7 and with the value of 89.89 MHz at 1.3 K from Ref. 5. The data reported in Fig. 4 correspond to the value $\nu(0)=89.90$. A different choice for $\nu(0)$ within 0.1 MHz does not produce relevant modifications to the plot.

The interesting feature which emerges is a power-law

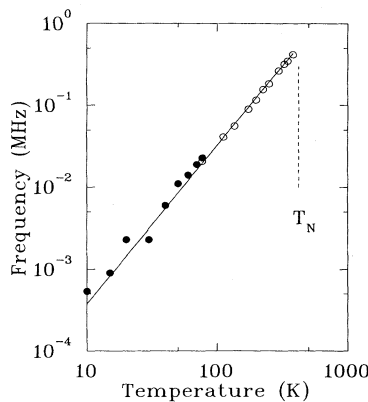


FIG. 4. Log-log plot of $(\nu_L(0)-\nu_L(T))/\nu_L(0)$. The solid line is the linear fit, corresponding to Eq. (2).

dependence of $\Delta\nu(T)/\nu(0)$ from 10 to 380 K. At low temperatures, an AT^α law with $A=6.83 \times 10^{-6} (\text{K}^{-\alpha})$ and $\alpha=1.87$ was already pointed out in Ref. 7. By using our values for ν_Q and ν_L the temperature dependence of the reduced magnetization is similarly described by AT^α with $A=(4.3 \pm 1.0) \times 10^{-6} (\text{K}^{-\alpha})$ and $\alpha=1.94 \pm 0.04$. The whole set of data can be well fitted by a unique expression

$$\Delta\nu(T)/\nu(0)=4.28 \times 10^{-6} T^{1.94} \quad (2)$$

throughout the entire temperature range between 10 and 380 K.

Although the Cu (2) signal itself cannot be followed up to the 3D Neel temperature, this transition may be directly determined on the same samples by means of a well defined peak in the $1/T_1$ relaxation of the Cu(1) nuclei. This peak is reminiscent of the one observed in a more conventional quasi-2D antiferromagnet, K_2MnF_4 ,¹³ at a fluorine site—the so-called F(2) site—where symmetry imposes zero contribution from the spin fluctuations at the antiferromagnetic mode. The $1/T_1$ peak was interpreted in that instance as a spill over of the slowing-down fluctuations, which produce a divergence of the relaxation rate at less symmetric sites. A similar picture applies here, where, likewise, Cu(1) is symmetrically placed with respect to the two sublattices and, in principle, it ought not to experience any net contribution. The resulting estimate of T_N for our sample is 420 K.

IV. THEORY AND DISCUSSION

The NMR data seem sufficiently precise and reproducible to allow a comparison with model calculations. As mentioned in the previous paragraph, the data are assumed to be directly proportional to the sublattice magnetization and the proportionality constant is also assumed to be temperature independent. If calculations are carried out within the frame of noninteracting spin-wave theory, the comparison is valid at low temperatures. For the present case, as it will appear in the following description, we will consider the calculation valid up to about 200 K.

The magnetic Cu^{2+} ions in $\text{YBa}_2\text{Cu}_3\text{O}_6$ are localized on two interpenetrating tetragonal sublattices.^{1,2} The sites of the a sublattice are $l\mathbf{a}_1+m\mathbf{a}_2+n\mathbf{a}_3$ where $\mathbf{a}_1=(a,0,0)$, $\mathbf{a}_2=(0,a,0)$, $\mathbf{a}_3=(0,0,c)$, a being the in layer nearest-neighbor (NN) distance. The sites of the b sublattice are shifted along the z axis by a vector $s\mathbf{a}_3$, with $s=0.28$. The layers sc distant are tightly bound and are referred to as double layer, the spin-spin exchange coupling being J_b . J_1 is the in layer NN exchange coupling between x and y spin components, while $(1-\eta)J_1$ couples the z components with $0 < \eta < 1$ in order to assure the XY easy-plane character of the exchange anisotropy. J' is the exchange integral along the c axis between spins that are $0.72c$ from each other. All exchange couplings are antiferromagnetic.

The model Hamiltonian reads

$$\begin{aligned}
\mathcal{H} = & -J_1 \sum_{i,\delta} (\mathbf{S}_i^{(a)} \cdot \mathbf{S}_{i+\delta}^{(a)} + \mathbf{S}_i^{(b)} \cdot \mathbf{S}_{i+\delta}^{(b)}) \\
& + \eta J_1 \sum_{i,\delta} (S_i^{(a)z} S_{i+\delta}^{(a)z} + S_i^{(b)z} S_{i+\delta}^{(b)z}) \\
& - J_b \sum_i (\mathbf{S}_i^{(a)} \cdot \mathbf{S}_{i+\delta_b}^{(b)} + \mathbf{S}_i^{(b)} \cdot \mathbf{S}_{i-\delta_b}^{(a)}) \\
& + J' \sum_i (\mathbf{S}_i^{(a)} \cdot \mathbf{S}_{i-\delta'}^{(b)} + \mathbf{S}_i^{(b)} \cdot \mathbf{S}_{i+\delta'}^{(a)}), \quad (3)
\end{aligned}$$

where $\delta = (\pm a, 0, 0)$, $(0, \pm a, 0)$, $\delta_b = (0, 0, 0.28c)$, and $\delta' = (0, 0, 0.72c)$. Define the reduced parameters

$$j_b = J_b / J_1, \quad j = J' / J_1.$$

In order to get the spin-wave spectrum we account for possible helix configurations characterized by the \mathbf{Q} wave vector both in a and b sublattice. The angle between NN a and b spins of a double layer is $\mathbf{Q} \cdot \delta_b + \theta$. The basic steps are standard:¹⁴ introduction of local quantization axis, Holstein-Primakoff or Dyson-Maleev transformation and Bogoliubov transformation. The minimum energy configuration evaluated in the classical limit ($S \rightarrow \infty$) is characterized by the wave vector $\mathbf{Q} = (\pi/a, \pi/a, 0)$ and $\theta = \pi$. This configuration agrees with that observed in $\text{YBa}_2\text{Cu}_3\text{O}_6$ by elastic neutron scattering.¹ The magnon dispersion curve in harmonic approximation is

$$\begin{aligned}
\hbar\omega_{\mathbf{k}}^{\pm} = & 8|J_1|S \left\{ \left[1 + \frac{1}{4}(j_b + j) - \frac{1}{2}(\cos ak_x + \cos ak_y) \mp \frac{1}{4}\sqrt{j_b^2 + j^2 + 2j_b j \cos ck_z} \right] \right. \\
& \times \left. \left[1 + \frac{1}{4}(j_b + j) + \frac{1}{2}(1 - \eta)(\cos ak_x + \cos ak_y) \pm \frac{1}{4}\sqrt{j_b^2 + j^2 + 2j_b j \cos ck_z} \right] \right\}^{1/2}. \quad (4)
\end{aligned}$$

The order parameter is given by the thermal average of the spin component along the local quantization axis

$$M(T) = S - \Delta S - \Delta S(T), \quad (5)$$

where

$$\Delta S = \frac{2}{N} \sum_{\mathbf{k}} \frac{1}{4} \left[\frac{A_{\mathbf{k}}}{\hbar\omega_{\mathbf{k}}^+} + \frac{A_{\mathbf{k}}}{\hbar\omega_{\mathbf{k}}^-} \right] - \frac{1}{2} \quad (6)$$

and

$$\Delta S(T) = \frac{2}{N} \sum_{\mathbf{k}} \frac{1}{2} \left[\frac{A_{\mathbf{k}}}{\hbar\omega_{\mathbf{k}}^+} \frac{1}{e^{\beta\hbar\omega_{\mathbf{k}}^+} - 1} + \frac{A_{\mathbf{k}}}{\hbar\omega_{\mathbf{k}}^-} \frac{1}{e^{\beta\hbar\omega_{\mathbf{k}}^-} - 1} \right] \quad (7)$$

with

$$A_{\mathbf{k}} = 8|J_1|S \left[1 - \frac{1}{4}\eta(\cos ak_x + \cos ak_y) + \frac{1}{4}(j_b + j) \right]. \quad (8)$$

Because of the high value of $|J_1|$ we perform the long-wavelength approximation with respect to k_x and k_y around $(0,0)$ and $(\pi/a, \pi/a)$ keeping the complete k_z dependence in order to evaluate the thermal demagnetization as given by Eq. (8). Taking advantage from the fact that $j \ll j_b$ we obtain

$$\Delta S(T) \simeq -\frac{t}{2\pi} \left\{ \ln(1 - e^{-\sqrt{j_b}/t}) + \ln(1 - e^{-\sqrt{2\eta+j_b}/t}) + \frac{2}{\pi} \int_0^\pi dz \left[\ln(1 - e^{-(\sqrt{j_b}/t)\sin z}) + \ln(1 - e^{-\sqrt{2\eta+j}\sin^2 z/t}) \right] \right\}, \quad (9)$$

where $t = k_B T / (8|J_1|S)$. Notice that t is only of the order 0.1 at the Néel temperature of $\text{YBa}_2\text{Cu}_3\text{O}_6$. In the limit $\eta, j \ll t$, which physically defines a quasi-2D system, the spontaneous reduced magnetization reads:

$$\frac{M(T)}{M(0)} \simeq 1 + \frac{t}{2\pi M(0)} \left[\ln(1 - e^{-\sqrt{j_b}/t}) + \ln(1 - e^{-\sqrt{2\eta+j_b}/t}) + \ln \frac{\sqrt{j}}{2t} + \ln \frac{\sqrt{2\eta+j}\sqrt{2\eta+j}}{2t} \right]. \quad (10)$$

From inelastic neutron-scattering data¹⁵ one has $8|J_1|S = 4000$ K, $j_b = 0.02$, $j = 3 \times 10^{-5}$, and $\eta = 1.5 \times 10^{-4}$. For this choice of parameters the analytic approximation (10) agrees within a few thousandth with Eqs. (9) and (7) for any temperature between 10 and 400 K. Moreover we have verified that $M(T)/M(0)$ is substantially independent of η and j_b , somewhat dependent on j and J_1 . Clearly we refer to Hamiltonian parameters within the experimental uncertainty.² We find $M(0) = S - \Delta S = 0.325$.

In Figs. 3 and 5 we compare the simple spin-wave expectation with our NMR data and with elastic neutron

scattering,¹ respectively; theory has been rescaled to each experiment multiplying the reduced magnetization by the $T=0$ extrapolation of the experimental curve. Both ENS and NMR are believed to measure the spontaneous magnetization in the ordered phase, so that they should agree, as it is the case, for instance, for the detailed measurements performed by these techniques in K_2NiF_4 (Refs. 16 and 17). As one can see in Fig. 3 the simple spin-wave theory seems to agree better with NMR data although the experimental uncertainty of the Hamiltonian parameters¹⁵ allows one to fit ENS data with the choice $8|J_1|S = 4400$ K for a large temperature range.

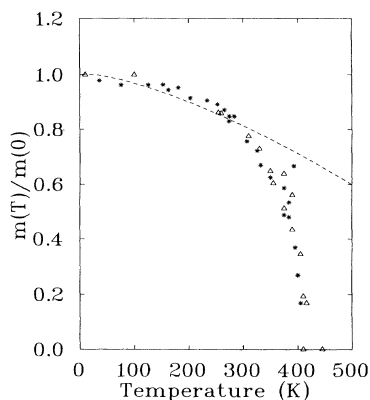


FIG. 5. Comparison between Eq. (10) (dashed curve) and the ENS data from Ref. 1.

This value is only 10% larger than the value that best fits NMR data, nevertheless this small disagreement needs to be further examined.

Recently, a good fit¹⁸ of the ENS data was given on the basis of a spin-wave approach where only thermal contributions involving optical magnons are neglected. Upon careful examination, it appears that our approach should agree with that of Ref. 18, given equivalent choice of coupling constants. However we have not been able to reproduce the curve of Fig. 1(b) in that paper; the results we obtain always give a greater reduction of magnetization with temperature, as reported in Fig. 5 of this paper. The discrepancy between our theoretical curve and that of Ref. 18, although not very large, is important because it is of the same magnitude of the difference between the ENS and NMR experimental data.

Strictly speaking this difference means that, despite the common natural assumption, the two techniques do not measure the same quantity. Looking at the relatively small difference between the two sets of data points in Figs. 3 and 5, this statement might sound excessive. It is however strongly supported by further observations on $\text{YBa}_2\text{Cu}_3\text{O}_{6+x}$ with $0.0 < x < 0.3$: ENS data show that between $x = 0.15$ and $x = 0.2$ the 3D magnetization decreases by at least 10%. On the contrary, NMR experiments at 4 K (Ref. 6) show that the Cu(2) NMR frequency and amplitude do not depend on oxygen content in this range, in agreement with our findings in the similar system, $\text{ErBa}_2\text{Cu}_3\text{O}_{6+x}$, also at higher temperatures, namely 77 and 293 K (Ref. 19) and with μSR results (Ref. 20) as well.

Actually, in the comparison of NMR with ENS, one must recall that local probes, such as NMR, which measures the local magnetic moment $\langle S_i \rangle$, may see something different from nonlocal probes, such as ENS, which samples the sum of a large number of sites of the same quantity $\sum_{i=1}^N \langle S_i \rangle$. It is clear that $\langle S_i \rangle \geq 1/N \sum_{i=1}^N \langle S_i \rangle$, the inequality being strictly valid if cancellations take place in the sum.

This indeed does happen in the range $x > 0.3$: ENS infers 3D stacking disorder^{1,2} from a loss of Bragg intensity and a concomitant additional scattering along lines

in q space, parallel to the c^* direction (rods). The intensity of the latter is significant in the whole ordered phase and it actually grows towards $T=0$. The very existence of such rods is well known for a variety of simple 2D antiferromagnets,¹⁶ their appearance being limited to the phase transition region. The presence of rods even at low temperatures in $\text{YBa}_2\text{Cu}_3\text{O}_{6+x}$ is a novel feature of these materials. The interpretation proposed by the authors in terms of static stacking disorder induced by the holes in the bilayers is, however, convincing.

How could these observations fit together? In such nearly two-dimensional antiferromagnets with thermally activated charge defects, we can envisage the formation of a quasi-two-dimensional domain structure, weakly correlated along the c axis. At low temperatures the domain borders within the planes are pinned by frozen defects and their imperfect stacking gives rise to a sizeable volume fraction occupied by the blurred walls. This structure contains the kind of static disorder which gives rise to ENS rods at $T=0$. It also implies an absolute difference between the magnetization measured from integrated Bragg peaks, reduced by the lack of coherence in the domain walls (the scattering from these regions goes in the rods), and that extracted from the NMR frequency, insensitive to large scale spatial coherence.

However the true issue is whether a difference in the temperature dependence detected by the two techniques is justified. Here we can only infer by analogy: ENS does observe a complicated temperature dependence of the rods' intensity at $x \geq 0.3$, accompanied by correspondingly unconventional behavior of the Bragg peaks (reentrance). The corresponding observations by NMR (Refs. 6 and 19) are sparse but indicate *normal* behavior. This implies that, when spin dynamics sets in and the amount of static disorder is altered by the activated hole motion, the Bragg peak intensity is sensitive to this varying amount of disorder, while NMR is not. Therefore the different sensitivity to a stacking disorder correlated with the hole position, together with a thermally activated hole mobility may lead to discrepancies also in the shape of ENS versus NMR curves. In turns the differences in the ENS and NMR data of Figs. 3 and 5 for $x \approx 0.00$ may originate from a mechanism as that of a pinned quasi-2D domain structure model. Recent findings on a similar system such as $\text{La}_{2-x}\text{Sr}_x\text{CuO}_{4+y}$ for $y \approx 0.00$ and $0 \leq x \leq 0.02$ (phase diagram and magnetic susceptibility²¹ and ¹³⁹La NQR data²²) indicate the presence of antiferromagnetic domains whose correlation length is limited by charge defects and give support to a pinned quasi-2D domain structure model.

An independent check of our picture would be the detection of static stacking disorder for $0 \leq x < 0.25$. Unfortunately a search for rods was not performed by ENS experiments for $x < 0.3$, probably because the low signal-to-noise ratio prevents it. Therefore differences in the NMR and ENS magnetization shape are the most sensitive way of checking these models.

Regarding the NMR data, the spin-wave model cannot be expected to reproduce the experimental data too close to T_N and from this point of view the incipient systematic deviations above $T=200$ K are not significant, still the

fact that the empirical fit to a power law (Fig. 4) agrees with all measured data, up to 380 K ($T/T_N=0.92$), is striking. No simple explanation is available for this peculiar behavior: It is well known that a T^2 law applies to 3D Heisenberg antiferromagnets, but certainly one cannot use this fit to seriously argue in favor of such interpretation for these nearly two-dimensional materials, as has been previously proposed.⁷ However the adherence to a simple analytical expression is remarkable and one might wonder whether the complete picture has indeed been achieved.

V. CONCLUSIONS

We believe that the magnetization curve extracted from Cu(2) NMR measurements is the best experimental

determination, to date, of the temperature dependence of the local magnetic moment in a highly deoxygenated $\text{YBa}_2\text{Cu}_3\text{O}_{6+x}$. Its comparison to simple spin-wave theory is satisfactory in the main. Small but significant deviations from ENS results are probably related to the existence of static as well as dynamical disorder in 3D stacking of the antiferromagnetic planes.

ACKNOWLEDGMENTS

We would like to thank Dr. C. Vignali for help with the Bruker spectrometer and Dr. F. Licci for the starting $\text{YBa}_2\text{Cu}_3\text{O}_7$ material. This work was partially supported by CNR Progetto Finalizzato Superconduttività and by INFM Project SAT.

-
- ¹J. Rossat-Mignod *et al.*, J. Phys. (Paris) Colloq. **49**, C8-2119 (1988).
²M. Jurgens, Ph.D. thesis, Leiden University, 1990.
³N. Nishida *et al.*, Jpn. J. Appl. Phys. **26**, L1856 (1987).
⁴Y. Kuno *et al.*, Phys. Rev. B **38**, 9276 (1988).
⁵H. Yasuoka *et al.*, J. Phys. Soc. Jpn. **57**, 2659 (1980).
⁶P. Mendels *et al.*, Physica C **171**, 429 (1990).
⁷Y. Iwamoto *et al.*, J. Phys. Soc. Jpn. **61**, 441 (1992).
⁸R. De Renzi *et al.*, Hyperfine Interact. **63**, 295 (1990).
⁹A. J. Millis *et al.*, Phys. Rev. B **42**, 167 (1990).
¹⁰E. Rastelli *et al.*, J. Appl. Phys. **69**, 4897 (1991).
¹¹G. M. Volkoff, Can. J. Phys. **31**, 820 (1953).

- ¹²M. Mali *et al.*, Physica C **175**, 581 (1991).
¹³C. Bucci and G. Guidi, Phys. Rev. B **9**, 3053 (1974).
¹⁴E. Rastelli *et al.*, J. Phys. Condensed Matter **2**, 8935 (1990).
¹⁵J. Rossat-Mignod *et al.*, Physica B **169**, 58 (1991).
¹⁶R. J. Birgeneau *et al.*, Phys. Rev. Lett. **22**, 720 (1969).
¹⁷H. W. de Wijn *et al.*, Phys. Rev. Lett. **24**, 832 (1970).
¹⁸B. Keimer *et al.*, Phys. Rev. B **45**, 7430 (1992).
¹⁹S. Jang *et al.* (unpublished).
²⁰D. R. Harshmann *et al.*, Phys. Rev. B **38**, 852 (1988).
²¹J. H. Cho *et al.*, Phys. Rev. Lett. **70**, 222 (1993).
²²J. H. Cho *et al.*, Phys. Rev. B **46**, 3179 (1992).